SPATIALLY RESOLVED LIFETIME INVESTIGATIONS OF Al- AND P-GETTERING IN COMBINATION WITH REMOTE HYDROGEN PLASMA PASSIVATION IN EFG RIBBON SILICON

P. Geiger, G. Kragler, G. Hahn, P. Fath, E. Bucher

Universität Konstanz, Fachbereich Physik, Fach X916, 78457 Konstanz, Germany
Tel.: +49-7531-88-2132, Fax +49-7531-88-3895, e-mail: patric.geiger@uni-konstanz.de

ABSTRACT: In defect containing silicon minority charge carrier lifetimes can be improved by gettering and passivation techniques in order to reach sufficient solar cell efficiencies. Consequently, such processing steps should be investigated. This has partly been done in this study, where the impact of P- and Al-gettering and their combination with a remote hydrogen plasma passivation on Edge-defined Film-fed Growth (EFG) silicon ribbons was examined. But in contrast to previous studies of other groups the mapping microwave detected photoconductance decay technique was applied for the measuring of lifetimes. As a consequence not just integral lifetime values but spatially resolved lifetime mappings have been obtained. This turned out to be essential for a detailed investigation of processing steps applied to EFG silicon material, as it was found that regions of comparable starting lifetimes can react very differently on the various processing steps. Therefore, the results of integral measurements depend strongly on the nature of regions incorporated in the specific sample. Moreover, it was found that the impact of the different processing steps on the various wafer areas also depends strongly on their starting quality. In good regions bulk lifetimes of about 280μm have been reached.
Keywords: Ribbon Silicon – 1: Lifetime – 2: Gettering – 3

1 INTRODUCTION

EFG ribbon silicon, as supplied by ASE Americas Inc., is grown directly out of the melt in the required thickness. In this way expansive sawing costs are avoided. According to the specific growth process, however, a certain amount of impurities and defects can be found in the material. A further possibility of reducing the module costs per Watt is therefore the reduction or passivation of these defects during cell processing. The development of such adequate processing schemes requires the investigation of the different processing steps' impact on the specific silicon material. This can be done, for example, by measuring the lifetime of minority charge carriers before and after processing steps, whereas one has to distinguish between integral ([1, 2]) and spatially resolved measurement techniques. In the case of EFG silicon which shows strong variations of material properties within few square centimeters (see e. g. [3]), it is not a priori clear that the different regions react in the same way and to the same extent to various processing steps. For that reason we have studied their response to standard processing steps in a spatially resolved way.

2 EXPERIMENTAL APPROACH

2.1 Measuring bulk lifetimes in EFG

The mapping of lifetimes within state-of-the-art p-doped EFG silicon ribbons (see [4]) was realized with the method of microwave detected photoconductance decay (μ-PCD). All measurements were performed under low injection conditions with a laser wavelength for charge carrier generation of 905 nm and bias light. In this way an effective lifetime τ_{eff} has been measured which can be calculated according to:

$$\frac{1}{\tau_{eff}} = \frac{1}{\tau_{bulk}} + \frac{1}{\tau_{surface}}$$

As we were interested in the bulk lifetime τ_{bulk} it was necessary to passivate the samples' surfaces so that the contri-

bution of $\tau_{surface}$ could be neglected. In this study this was achieved by the use of a iodine-alcohol solution. Therefore, it was possible to investigate the impact and synergetic effects of different processing steps on the same sample by measuring the resulting change in bulk lifetime with the help of a reproducible surface passivation.

The determination of τ_{eff} or τ_{bulk} from the decay of photoconductance requires the selection of an adequate time range in which the decay is evaluated. But due to the strong variations of material quality within EFG wafers it is usually not possible to choose a single time range well-suited for the whole sample. This problem was addressed by measuring each wafer partly or as a whole for several times with different time ranges. The resulting data was finally combined in an adequate way with the help of developed software procedures. As a consequence rather low lifetime values as well as quite high ones are reliable in the mappings shown in this study.

2.2 Design of experiment

The experiment was devided into four processing sequences represented by the four columns shown in Fig. 1. At the beginning of the investigations 20μm were removed on each side of the wafers using an acid etching solution in order to obtain comparable surfaces. Before each measuring step indicated in the different columns the samples were chemically cleaned and their surface was passivated with an iodine-alcohol solution. POCl$_3$ phosphorous diffusion was performed in a quartz tube furnace the aluminium needed for gettering was evaporated. P-emitter as well as back surface field (BSF) were etched back before subsequent measurements in order to avoid recombination in the emitter or problems with surface passivation on the back side during μ-PCD measurement. A hydrogenation step was realized with the help of a microwave induced remote hydrogen plasma (MIRHP, [5]) and, as well as an illumination for ten hours under one sun, implemented according to the schematic drawing given in Fig. 1.
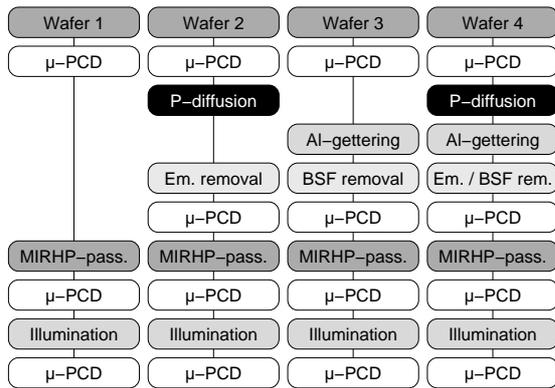
Figure 1: Structure of the experiment. After various successive processing steps spatially resolved bulk lifetime measurements have been performed.

3 RESULTS

After combining several measurements as described in section 2.1 mappings have been obtained which show reliable lifetime values in regions of quite good performance as well as in such of rather low lifetime. Those of wafer 2 are shown representatively in Fig. 2. Nevertheless, there is a region in mapping (a) of this figure where the measurement was not totally reliable. Consequently, those points, which are located in the best area of the mentioned mapping (at the centre of the bottom), were not taken into account and are marked with grey points. They can be seen even more clearly in the first illustration of the right column because of a better contrast. In all the following mappings, however, this problem has been solved so that there is no region of unreliable measurement points left.

3.1 Obtained mappings

The left column of Fig. 2 shows the bulk lifetime of the second wafer's minority charge carriers after the various processing steps given in Fig. 1. The right column, instead, contains mappings that have been generated by subtracting the data of the previous measurement from the relevant one, e. g. $(b) - (a)$. Having a closer look at the pictures (a) and (b) or rather $(b) - (a)$ one finds that P-gettering leads to strong improvements in areas of quite good starting lifetimes of about seven or more microseconds. Partly gains of up to $100\mu s$ have been measured. But things look different for areas of lower starting lifetimes. In such regions improvements of up to only $2\mu s$ have been measured, in numerous cases even much less. During the MIRHP-passivation again the areas with rather high starting lifetimes improve most strongly with a gain of up to $120\mu s$. But there are also a few small areas at the top of mapping (b) or $(c) - (b)$ where lifetime enhancements above $100\mu s$ have been measured although these regions had shown lifetime values lower than $4\mu s$ at the beginning. In contrast to P-gettering MIRHP hydrogenation also effects most of the areas with a worse performance and improves their lifetimes on average by about $20\mu s$. A further measurement after ten hours of illumination under one sun has revealed the MIRHP-passivation to be stable under illumination, as can be seen in mapping (d). The
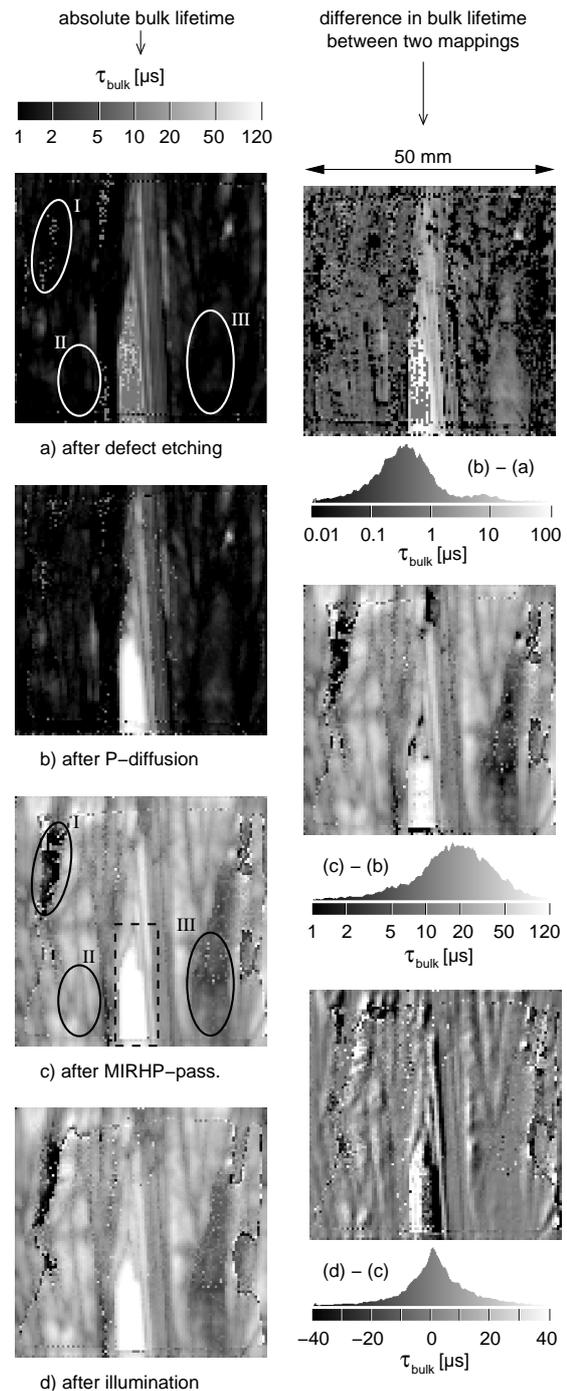

Figure 2: Bulk lifetime mappings of wafer 2 as obtained after appropriate combination of various measurements that lead to reliable high and low lifetime values. Left column shows the bulk lifetimes measured after different processing steps with all mappings scaled in the same way. Differences between two steps are illustrated by the right column.

differences given in $(d) - (c)$ are in most cases in the range of the measurement technique's accuracy. Whether the different reaction of the left and right part of the best region on illumination can be explained in this way is not quite clear yet, although the lifetimes in this region have been found to
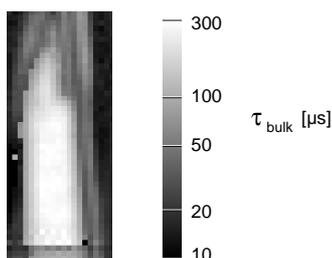
Figure 3: Differently scaled clipping of the region marked with a dashed box in Fig. 2(c).

be very high reaching up to $300\mu s$ as can be seen in Fig. 3. Perhaps a material analysis will help to answer this question in the future.

However, the most important aspect visible in Fig. 2 is that regions of comparable as grown lifetimes do exist within EFG wafers which are influenced differently by the various processing steps. And this has also been found in other wafers of Fig. 1. The marked region II of wafer 2, for example, improves significantly during hydrogenation, whereas lifetimes in region III remain rather low, although it has shown the same starting lifetimes and even slightly better lifetime values after P-diffusion than area II. Moreover, the marked region I includes an area with about the same starting lifetimes as those mentioned previously but which has hardly improved during all the different processing steps. Due to the existance of such regions of different behaviour and their inhomogeneous distribution according to usual wafer sizes integral lifetime measurement techniques appear to not to be well suited for a precise analysis. The results depend strongly on the nature of the regions incorporated in an examined sample and their share of the whole wafer. As a consequence a spatially resolved measurement technique should be used for detailed investigations.

3.2 Evaluation of histograms

For a very simple comparison of the impact of the applied processing steps it is possible to evaluate the histograms of lifetime mappings belonging to the different wafers of Fig. 1. In this way the subtleties described in section 3.1 are obviously not fully taken into account. But as the histograms contain some information about the lifetime distribution within in the sample they provide at least a few more details than an integral measurement.

The histograms of wafer 1 given in Fig. 4 illustrate that an acid defect etching step does not really influence the lifetime distribution. The MIRHP-passivation instead, has a significant impact on the minority charge carrier lifetimes which have been shifted from about $1\mu s$ to $10\mu s$. However, it is visible that the hydrogenation without a preceeding gettering step is not completely stable under illumination. The distributions belonging to wafer 2 look somewhat different: First, the histogram of the measurement after defect etching is much smaller and higher than in the case of wafer 1. It is slightly shifted to higher values by the P-diffusion step, but details like strong lifetime enhancements within regions of starting lifetimes above $7\mu s$ etc., which have been discussed in section 3.1, are not visible. A significant enhancement by hydrogenation, instead, can be seen clearly. Moreover,
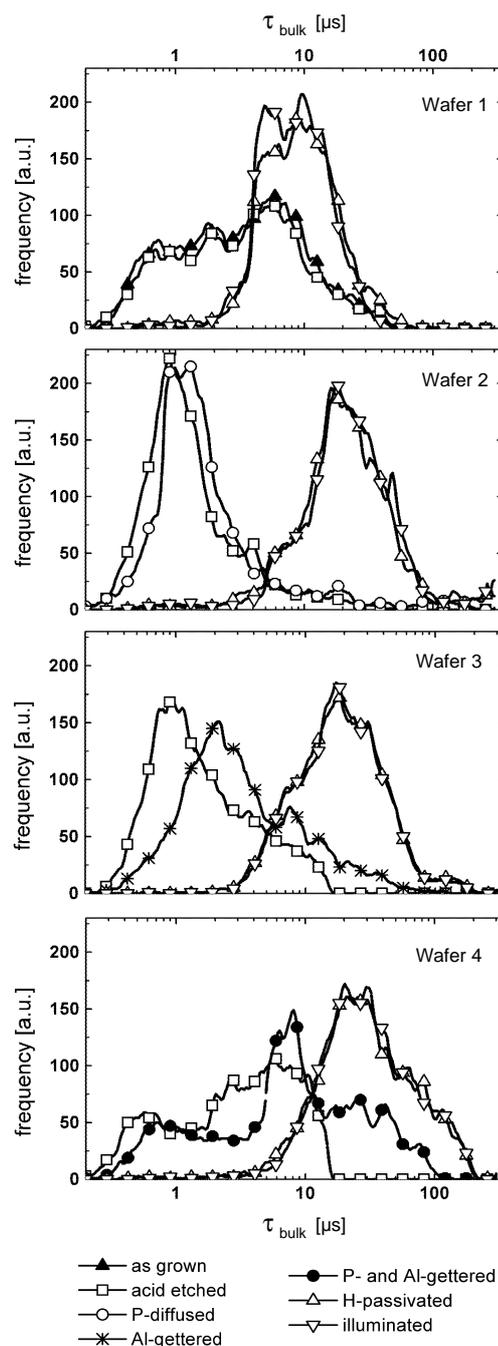

Figure 4: Histograms of bulk lifetime mappings performed on different wafers according to the schematic drawing in Fig. 1.

this step appears to be more efficient than without a preceeding P-gettering step (like in the case of wafer 1) and to be stable under illumination. This is also true in the case of Al-gettering represented by wafer 3. Again MIRHP-passivation is more efficient than without previous gettering and stable under illumination. As this sample shows a similar distribution of starting lifetime as wafer 2 the impact of the different gettering steps can be compared to each other within the restrictions of the loss of spatially resolved information. Doing so, one finds Al-gettering to be more efficient than P-

gettering. After hydrogen passivation, however, this difference is not visible any longer. Similar comparisons of the P-Al-gettering step with the help of histograms are not possible as wafer 4 shows a distribution of starting lifetimes very different to those of wafers 2 and 3. But again, as one supposes after the results of wafer 2 and 3, the hydrogenation is stable under illumination. Furthermore, the final lifetime values are in the same range as those of the other gettered wafers, so that gettering once more seems to improve the efficiency of a following MIRHP hydrogenation step. For more detailed information, however, one has to refer to the lifetime mappings, break them up into regions of similar starting lifetimes and analyze them.

SUMMARY

In this study it has been shown that Al-gettering has a more benefical influence on the bulk lifetime of minority charge carriers in EFG silicon ribbons than P-gettering, although there is no much difference left if a microwave induced remote hydrogen plasma passivation follows the gettering steps. This H-passivation has been found to be stable if a P- oder Al-gettering step or both precede the hydrogenation. Otherwise it is not totally stable and much less efficient.

Furthermore, it has been shown that there exist regions of comparable starting lifetimes within EFG silicon which react very differently on the various solar cell processing steps. Some improve very strongly reaching high lifetimes, others are only insufficiently enhanced. As such areas are inhomogeneously distributed according to usual wafer sizes they influence integral lifetime measurements so that a detailed analysis requires a spatially resolved lifetime measurement technique.

Future work will address the question of the nature the defects in these different regions in order to find out the reasons for their behaviour and a way to improve those areas which are not enhanced sufficiently by gettering and passivation at the moment.

ACKNOWLEDGEMENT

REFERENCES

[1] A. Rohatgi, V. Yelundur, J. Jeong, A. Ebong, D. Meier, A. M. Gabor, M. D. Rosenblum, Proc. 16th EC PVSEC, Glasgow, UK (2000) 1120.

[2] J.-W. Jeong, A. Rohatgi, M. D. Rosenblum, J. P. Kalejs, Proc. 28th IEEE PVSC, Anchorage, Alaska (2000) 83.

[3] P. Geiger, G. Hahn, P. Fath, E. Bucher, to be published in Sol. En. Mat..

[4] B. Bathey, J. Kalejs, M. Rosenblum, M. Kardauskas, R. Giancola, J. Cao, Proc. 28th IEEE PVSC, Anchorage, Alaska (2000) 194.

[5] M. Spiegel, P. Fath, K. Peter, B. Buck, G. Willeke, E. Bucher, Proc. 13th EC PVSEC Nice, France (1995) 421.